

---

This is an electronic reprint of the original article.  
This reprint may differ from the original in pagination and typographic detail.

Martinovski, Tatjana; Sourander, Tom; Turunen, Aleks; Minav, Tatiana; Pietola, Matti  
**Control strategy for a direct driven hydraulics system in the case of a mining loader**

*Published in:*  
11th International Fluid Power Conference, Aachen, Germany

*DOI:*  
[10.18154/RWTH-2018-224472](https://doi.org/10.18154/RWTH-2018-224472)

Published: 01/01/2018

*Document Version*  
Publisher's PDF, also known as Version of record

*Please cite the original version:*  
Martinovski, T., Sourander, T., Turunen, A., Minav, T., & Pietola, M. (2018). Control strategy for a direct driven hydraulics system in the case of a mining loader. In H. Murrenhöf (Ed.), *11th International Fluid Power Conference, Aachen, Germany* (Vol. 1, pp. 294-305). RWTH Aachen University. <https://doi.org/10.18154/RWTH-2018-224472>

---

This material is protected by copyright and other intellectual property rights, and duplication or sale of all or part of any of the repository collections is not permitted, except that material may be duplicated by you for your research use or educational purposes in electronic or print form. You must obtain permission for any other use. Electronic or print copies may not be offered, whether for sale or otherwise to anyone who is not an authorised user.



## Control strategy for a direct driven hydraulics system in the case of a mining loader

Tatjana Martinovski, Tom Sourander, Alekski Turunen, Tatiana Minav and Matti Pietola

Aalto University, Department of Mechanical Engineering, Otakaari 4, 02150 Espoo, Finland  
E-Mail: tatjana.martinovski@aalto.fi

As a response to the strict government emissions regulations, hybridisation of non-road mobile machinery is required. In this paper, behaviour and efficiency of a hybrid mining loader is studied. The full prototype with implemented DDH (Direct Driven Hydraulics) units had been built; however, its performance was unsatisfactory – a large undershoot and steady-state error of 34 % persisted. Therefore, a new control strategy was suggested to overcome the issues. Performance of the system was enhanced by applying a fuzzy PID controller. As a result, reference tracking was significantly improved compared to the conventional PID control case and steady-state error of 1 % was achieved, while the overall efficiency was kept high in the range of above 50%.

**Keywords:** fuzzy control, direct driven hydraulics, mining loader, efficiency

**Target audience:** Mobile Hydraulics, Mining Industry, Control

### 1 Introduction

The problem of air pollution is becoming more and more severe, and especially non-road mobile machinery (NRMM) contributes to this pollution by emitting considerable amounts of nitrogen oxides and particulate matter into the air [1]. Stricter emissions regulations have been proposed [2], and in order to comply with them and decrease energy consumption, the hybridisation of NRMMs is essential. One of the solutions for the hybridisation of such machinery lies in replacing the traditional working hydraulics with a Direct Driven Hydraulics (DDH) setup. In DDH, a hydraulic pump is powered by an electric motor, and it directly controls the actuator [3]. The usage of an electric motor provides shorter response time, which also improves efficiency by reducing losses. Since conventional valve control is not utilized, throttle losses are avoided and heat generation is reduced.

Mining loaders, large NRMMs used in the mining industry, have been the target of such hybridisation. For instance, the conventional hydraulic system of a mining loader was replaced with DDH during the Tubridi project [4], and basic expectations concerning its functionality were met. However, the control of the system was unsatisfactory, as the movements of the machine during its working cycle were insufficiently smooth and the error of 34% of the reference position was present during the EL-Zon project (in the case of 1040 kg payload). Furthermore, it was necessary to retune the controller with each change in the payload. Moreover, there was room for improvement in the overall energy efficiency of the system. In order to overcome these problems, the present study suggested to utilise a different control method. Due to complexity of the system and its high nonlinearities, fuzzy PID control was chosen, as a highly accurate mathematical model is not necessarily needed for designing this type of control. This control technique has already been implemented in a number of hydraulic and electro-hydraulic systems, and it has proven suitable for such application [5 - 7].

Therefore, this study aims to develop new control strategy in order to overcome issues, such as the need of retuning the PID controller with each change of payload and large steady-state error in reference tracking. The study evaluates validity of the proposed fuzzy PID controller using the test setup assembled during the Tubridi project (of which the present study is a continuation), and the results demonstrate improvement in energy efficiency and general behaviour of the system.

This paper is organized in the following way: first, Section 2 briefly introduces the test setup; second, Section 3 explains the basics of fuzzy control and its implementation in this specific case; then, Section 4 illustrates results and finally, Sections 5 and 6 present the discussion and conclusions, respectively.

### 2 Test setup

This section introduces the full-size mining loader prototype utilised in this experiment. The original working hydraulics of the EJC 90 mining loader (Figure 1) had been replaced with the DDH setup during the Tubridi and EL-Zon projects. The original hydraulic transmission was replaced with a fully electromechanical one. The diesel engine is not mechanically connected to the drive train, which makes its architecture series hybrid. It produces electric power, which is then buffered with a li-ion battery. The DDH setup consists of two separate units. One of them is utilised for boom movement control, while the other handles the bucket. The only difference between the two units is that the boom unit consists of two double-acting cylinders, whereas only one is present in the bucket unit, as can be seen in Figure 2. For more details about the setup, please refer to [4]. The utilised components of DDH units are demonstrated in Figure 2 and Table 1, for more details please refer to [8].

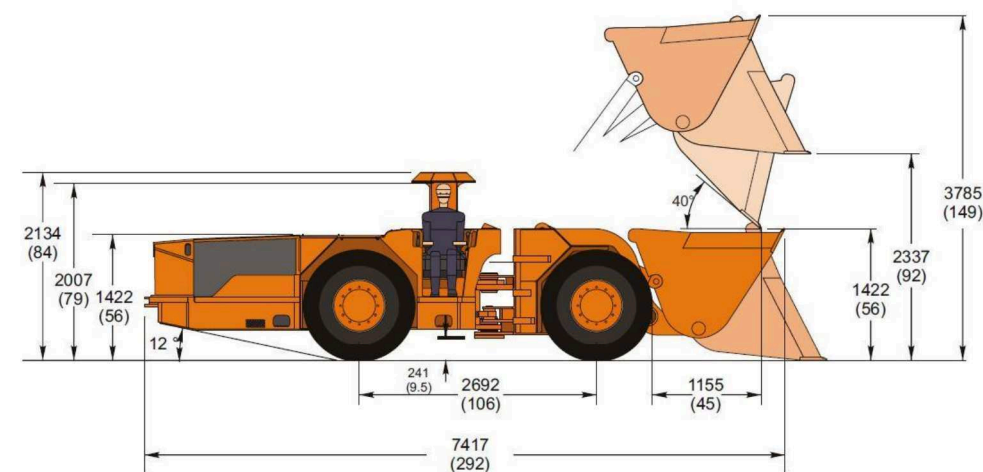


Figure 1: EJC 90 mining loader with dimensions in centimetres and inches

In DDH, the speed of the electric motor defines the flow produced by the hydraulic motors, hereafter referred to as *pumps*, which then determines the flow to the cylinder chambers. The pumps are connected to the motor shaft via a gearbox. Speed and torque data from the electric motor is utilised by dSPACE control desk software to control the basic movements of the bucket and the boom. The program either receives user input via a joystick (manual mode) and performs the movement or executes a given cycle (automatic mode).

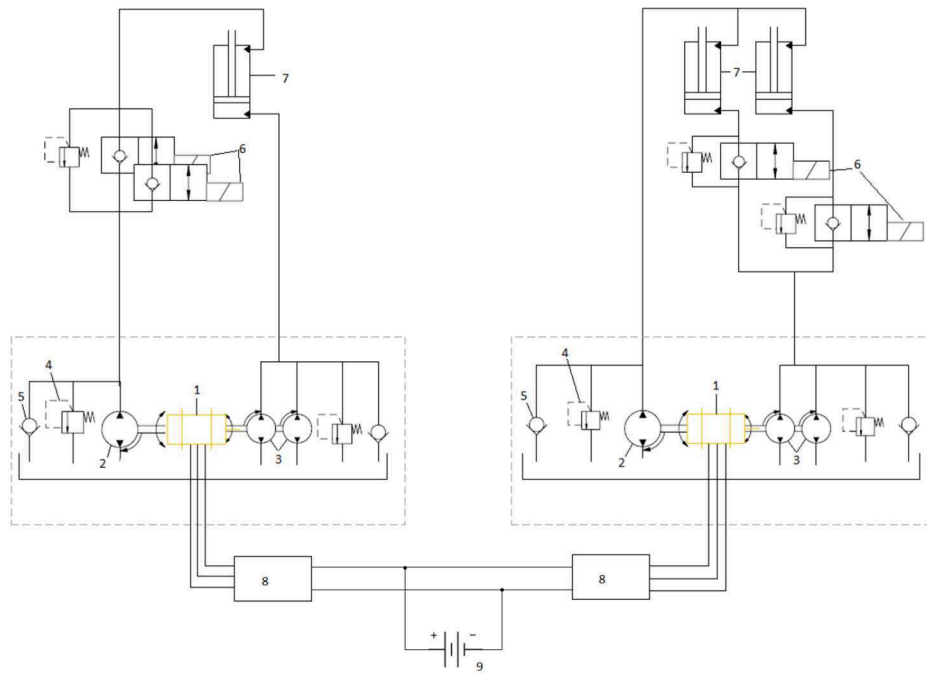


Figure 2: Models of DDH units of bucket (left) and boom (right)

	Component	Model	Additional information
1	Electric motor	Motenergy ME1304	
2	B-side pump	HYDAC PGI100	Boom: PGI100-013+011; Bucket: PGI100-022x2
3	A-side pumps	HYDAC PGI100	Boom: PGI100-008x2 X2; Bucket: PGI100-016x2 X2
4	Pump pressure relief valve	HYDAC DB10P-01	
5	Anti-cavitation valve	HYDAC RV12A-01	
6	Safety valves	HYDAC WS16ZR-01	
7	Hydraulic cylinder	EJC90 original	
8	Motor controller	Sevcon Gen 4	Size 6; DC/AC converter
9	Lithium-titanate battery	Altairnano 96V	

Table 1: Components of bucket and boom DDH units [Courtesy of T. Lehmuspelto. Aalto University. 2016]

The system diagram is illustrated in Figure 3. The grey lines on the diagram correspond to the signals sent via a CAN bus. The joystick is connected via the CAN bus to the dSPACE control desk program. For monitoring purposes dSPACE program also receives basic information about the battery (its state of charge, voltage, current). The reference signal is then sent via the CAN bus to the Sevcon DC/AC motor controllers, which are powered by the battery. Sevcon motor controllers control the boom and bucket electric motors. The boom electric motor is in speed-control mode, while the bucket electric motor operates in torque-control mode. The information about

motors' acting speed, torque and temperature is fed back to the Sevcon motor controllers. The motors are connected to the hydraulic system as shown in Figure 2. The dSPACE program receives information about cylinder position, temperature and pressure from the sensors and collects data about the hydraulic system. The reference tracking of the cylinder position is accomplished by the fuzzy PID controller, whose working principle is described in detail in the next section.

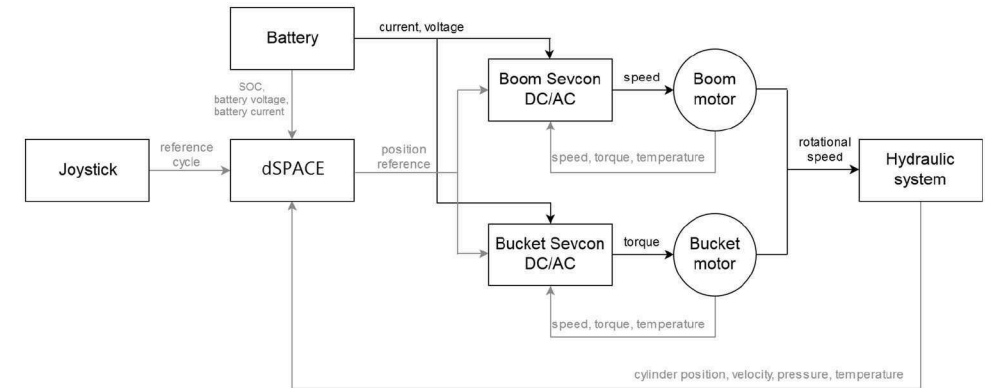


Figure 3: Block diagram of the system

### 3 Fuzzy PID control

In this section, basics of conventional PID and fuzzy PID controllers are discussed.

The well-known discrete-time transfer function of a PID controller is expressed by the following equation:

$$u(k) = K_p e(k) + K_i T_s \sum_{i=1}^n e(i) + \frac{K_d}{T_s} \Delta e(k) \quad (1)$$

where  $K_p$ ,  $K_i$  and  $K_d$  are proportional, integral and derivative gains, respectively,  $T_s$  is the sampling period,  $u(k)$  is the control signal, while  $e(k)$  is the error between the reference and the process output signal;  $\Delta e(k) = e(k) - e(k-1)$ . These parameters need to be determined, which can be rather challenging, especially in case of a hydraulic system. Inherent excessive nonlinearities and time-variant characteristics are present and, therefore, a control method based on a linear model, such as a PID controller, does not provide adequate results.

In order to improve the behaviour and efficiency of the system, a new self-tuning control strategy was implemented based on the fuzzy algorithm. Due to complexity of the system and its high nonlinearities, fuzzy PID control (Figure 4) was chosen. In this study, the parameters were selected according to the gains of previously used PID controllers and by trial and error testing. The control works as follows: position error (real position subtracted from the reference) and its derivative (velocity) are fed into the fuzzy block. It then calculates the gains of parameters according to predefined rules, which are then sent to the PID controller. The controller is implemented within the MATLAB Simulink real-time model.

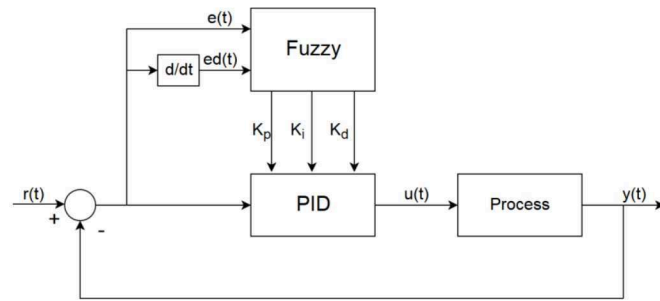


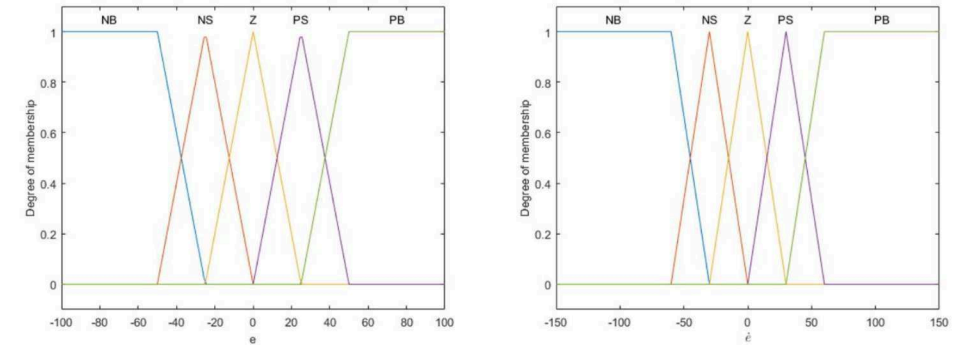
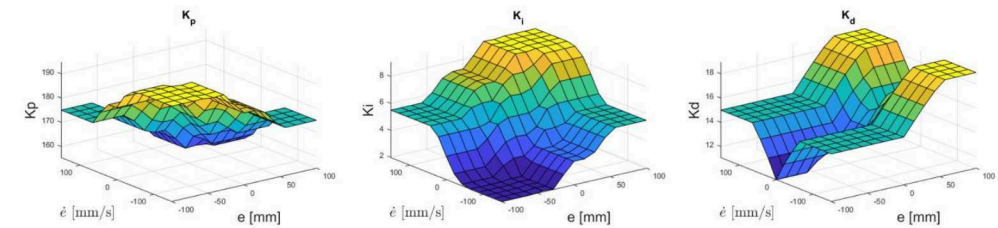
Figure 4: Fuzzy PID controller structure

The ranges of input variables are  $[-100, 100]$  for  $e$  in [mm] and  $[-150, 150]$  for  $\dot{e}$  in [mm/s]. These variables represent cylinder position error and its derivative – velocity, respectively. In the process of fuzzification, firstly, it is determined to which degree inputs belong to the fuzzy sets, via linguistic values – membership functions [9], defined as:  $e, \dot{e} = [NB, NS, Z, PS, PB]$ . The abbreviations stand for negative big, negative small, zero, positive small and positive big, respectively. Negative big and positive big are trapezoid-shaped functions, while the remainder is triangular (Figure 5). Then, fuzzy operator is applied (*minimum* as AND method and *maximum* as OR method) to the rules, which are given in Table 2. After that, the implication method (*minimum* in this case) is implemented, and the result is a fuzzy set represented by a membership function. Next step is aggregation, the phase in which all the rules are combined in order to make a decision (the aggregation method used is *maximum*). Finally, defuzzification is applied, and its result is a single number. “Centroid” was chosen as the defuzzification method. There exist five membership functions for fuzzy outputs:  $K_p, K_i, K_d = [VS, S, M, B, VB]$ , where the abbreviations stand for very small, small, medium, big and very big, respectively. The ranges of the parameters are:  $K_p = [150, 200]$ ,  $K_i = [1, 10]$  and  $K_d = [10, 20]$  for the boom control and  $K_p = [5, 10]$ ,  $K_i = [1, 3]$  and  $K_d = [3, 5]$  for the bucket control. The parameter ranges are tuned independently. Table 3 Table 2 contains the parameters of the membership functions of the controller outputs. Mamdani’s fuzzy inference method was adopted.

$K_p / K_i / K_d$	$\dot{e}$					
$e$		NB	NS	Z	PS	PB
	NB	VB / VS / M	VB / VS / S	B / S / VS	B / M / S	M / M / M
	NS	VB / VS / M	B / S / S	B / M / S	M / M / S	S / M / M
	Z	B / S / M	M / S / S	M / M / S	M / B / S	S / B / M
	PS	B / S / B	M / M / M	S / M / M	S / B / M	VS / VB / B
	PB	M / M / VB	S / M / B	S / B / M	VS / VB / B	VS / VB / VB

Table 2: Rule table of the fuzzy inference system

Figure 6 illustrates data from Table 2: it shows control surfaces of the parameters ( $K_p, K_i, K_d$ ) of the boom fuzzy PID. It can be seen from the table that the control surface of the bucket fuzzy PID parameters has exactly the same shape, since the rules are identical. The ranges of parameters are scaled to match the corresponding data from Table 3.

Figure 5: Membership functions of the controller input variables – position  $e$  and velocity error  $\dot{e}$ Figure 6: Control surface of the  $K_p, K_i$  and  $K_d$  parameters of the boom fuzzy PID

	VS	S	M	B	VB
$K_{p\_boom}$	[132 148 155 165]	[155 165 175]	[165 175 185]	[175 185 195]	[185 195 202 218]
$K_{i\_boom}$	[-2.24 0.64 1.9 3.7]	[1.9 3.7 5.5]	[3.7 5.5 7.3]	[5.5 7.3 9.1]	[7.3 9.1 10.36 13.24]
$K_{d\_boom}$	[6.4 9.6 11 13]	[11 13 15]	[13 15 17]	[15 17 19]	[17 19 20.4 23.6]
$K_{p\_bucket}$	[3.2 4.8 5.5 6.5]	[5.5 6.5 7.5]	[6.5 7.5 8.5]	[7.5 8.5 9.5]	[8.5 9.5 10.2 11.8]
$K_{i\_bucket}$	[0.28 0.92 1.2 1.6]	[1.2 1.6 2]	[1.6 2 2.4]	[2 2.4 2.8]	[2.4 2.8 3.08 3.72]
$K_{d\_bucket}$	[2.28 2.92 3.2 3.6]	[3.2 3.6 4]	[3.6 4 4.4]	[4 4.4 4.8]	[4.4 4.8 5.08 5.72]

Table 3: Parameters of the membership functions of the controller outputs

#### 4 Experimental investigation: results

Experimental investigation was performed on the full-size prototype described in section 2. A cycle was utilised to simulate the real operation of a mining loader. In Figure 7 references for boom and bucket position are demonstrated, as well as overall efficiency and regeneration efficiency (example data). The graphs are divided into sections with vertical lines in order to demonstrate the distinct stages of the cycle. (It should be noted that in the graph that represents bucket position, the highest value corresponds to the lowest bucket position and vice versa.) The cycle sequence where first, the (loaded) bucket is lifted to its upmost position (1-3), the boom is then lifted (4-5), next the bucket performs a “dropping” movement while the boom is resting (6-9), then the boom is lowered to the ground (10-11) and, finally, the bucket is lowered to the starting position (12-13). From this figure, it should be noted that highest efficiency level is present during lifting of the boom (4), while power regeneration is present during lowering of the boom (10). The equations utilised for calculating efficiency and regeneration efficiency are

given below, and Figure 8 demonstrates example data used in those calculations. Figure 8 corresponds to performed cycle that is presented in Figure 7.

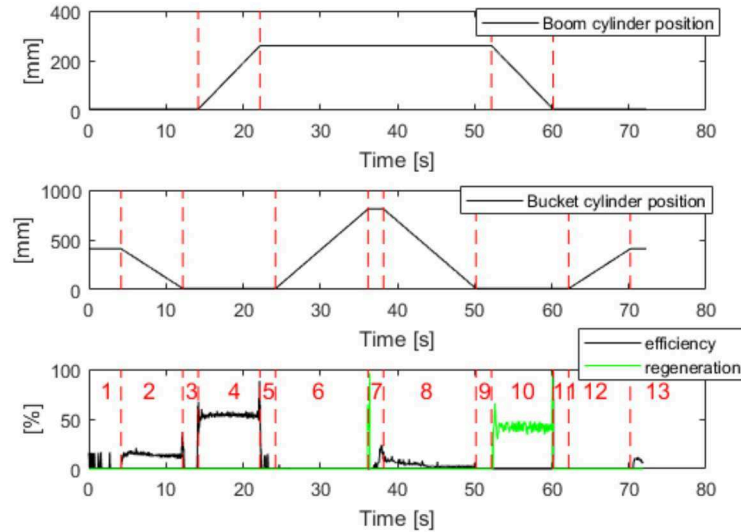


Figure 7: Example data of boom and bucket cylinder positions and overall efficiency and regeneration efficiency with distinct parts of the cycle

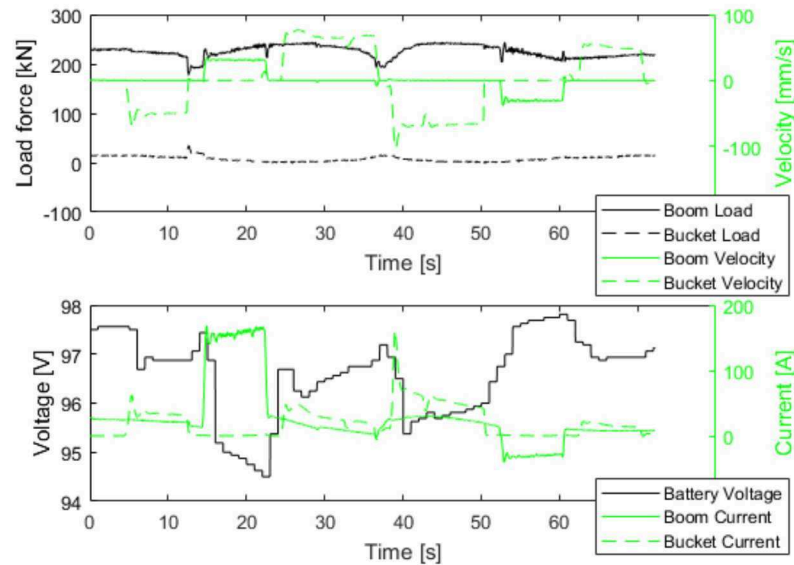


Figure 8: Example data utilised to calculate efficiency and regeneration efficiency

The major difference in the utilised cycle compared to real-life is that the payload is not dropped, due to conditions in the laboratory. The measurements were obtained without and with two different payloads – 1040 and 2080 kg. In further text, they are referred to as “no load”, “half-load” and “full load”, respectively. Moreover, four various

cylinder velocities were utilised. “Nominal cylinder velocities” in this context refers to the velocities that are defined by the position reference table (input cycle).

The overall system efficiency  $\eta$  that was calculated as the ratio of mechanical power  $P_{mech}$  and battery output power  $P_{bat}$ :

$$\eta = \frac{P_{mech}}{P_{bat}} \quad (2)$$

The regeneration efficiency  $\eta_{reg}$  was defined as ratio of battery and mechanical power (in this case, mechanical acts as input power, while battery power is understood as output, as power generated due to dynamic braking gets stored in the battery):

$$\eta_{reg} = \frac{P_{bat}}{P_{mech}} \quad (3)$$

In the Equations (2) and (3), mechanical power was calculated as:

$$P_{mech} = F_{boom}v_{boom} + F_{bucket}v_{bucket}, \quad (4)$$

where  $F_{boom}$  and  $F_{bucket}$  are forces acting on load pins of the boom and the bucket, respectively, while  $v_{boom}$  and  $v_{bucket}$  are cylinder velocities of the boom and the bucket, respectively. Battery power was calculated as:

$$P_{bat} = U_{bat}I_{boom} + U_{bat}I_{bucket}, \quad (5)$$

where  $U_{bat}$  is battery voltage and  $I_{boom}$  and  $I_{bucket}$  are battery current measured by the boom and bucket motor controller, respectively. Example of data needed for these calculations is shown in Figure 8, from which it can be seen that the load force and current measurements are highly oscillating, therefore oscillations and peaks are present in power and efficiency graphs. During the performed cycle, fluctuation of the current consumed by DDH units comes as a response to the required load. Negative values of current during lowering phase of the boom corresponds to regenerative energy, which is charging the battery (increase in state of charge is present).

It should be noted that even though fuzzy PID has been implemented for both boom and bucket control, the focus of this study was on boom reference tracking. Therefore, only boom position graphs are demonstrated in this paper. However, the efficiency is calculated and shown for the overall system, including both boom and bucket units.

An example of previous unsatisfying results with the conventional PID control is demonstrated in Figure 9.

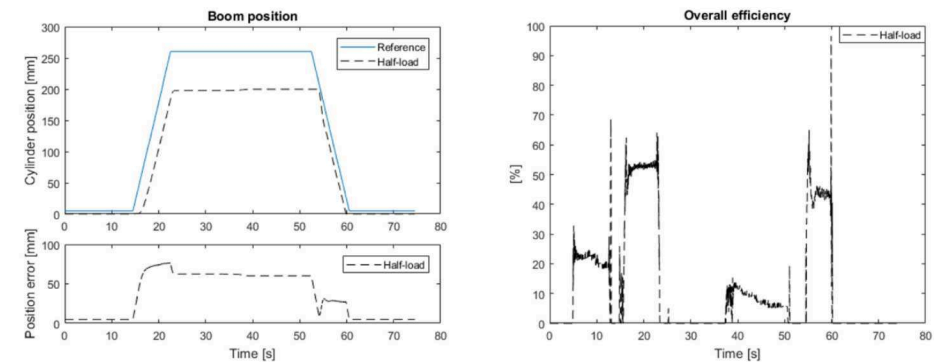


Figure 9: Experimental results: conventional PID – nominal cylinder velocity, half-load – boom position reference tracking (left, up), boom position error (left, down) and efficiency (right)

The fundamental issue with the conventional PID control was a fairly huge undershoot: the boom used to reach only 76 % of the reference, which corresponds to the steady-state error of 34 %. The main reason for such large error was that the controller was tuned for one specific weight of payload. Therefore, it either had to be retuned

with each change of payload, or the steady-state error in the position reference tracking persisted, which is one of the main reasons why this study was done. The efficiency level for this example case was around 52 %. To overcome the issues existing with the conventional PID controller, fuzzy PID was designed. The experimental results with the proposed fuzzy PID control are presented below in Figure 10 - Figure 13.

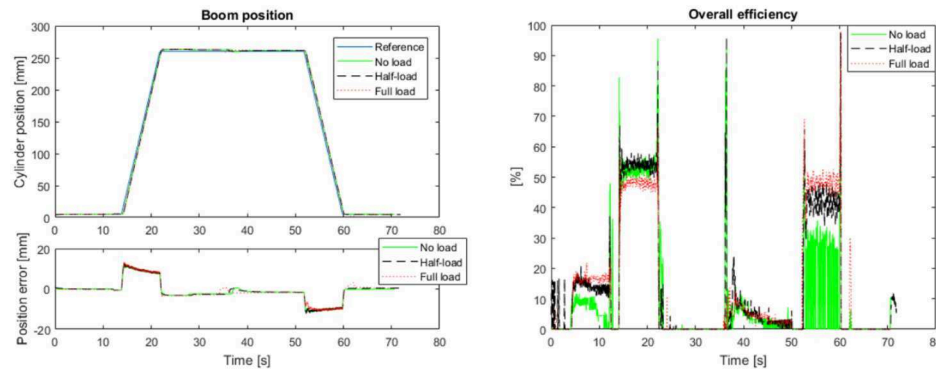


Figure 10: Experimental results: nominal cylinder velocity – boom position reference tracking (left, up), boom position error (left, down) and efficiency (right) for different payloads

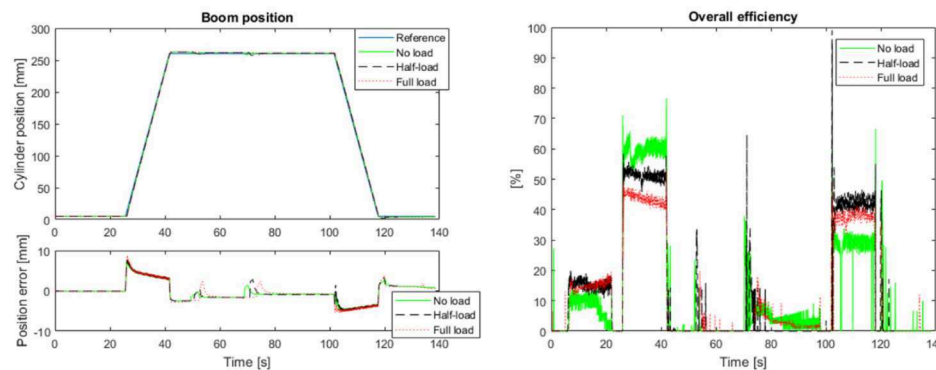


Figure 11: Experimental results: 0.5 \* nominal cylinder velocity – boom position reference tracking (left, up), boom position error (left, down) and efficiency (right) for different payloads

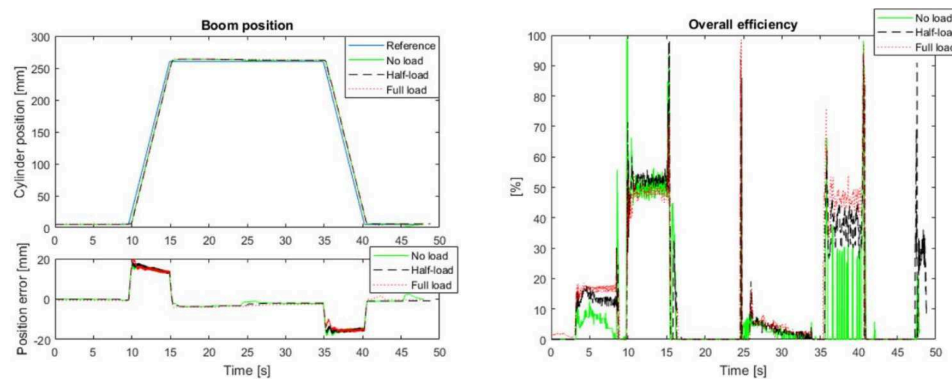


Figure 12: Experimental results: 1.5 \* nominal cylinder velocity – boom position reference tracking (left, up), boom position error (left, down) and efficiency (right) for different payloads

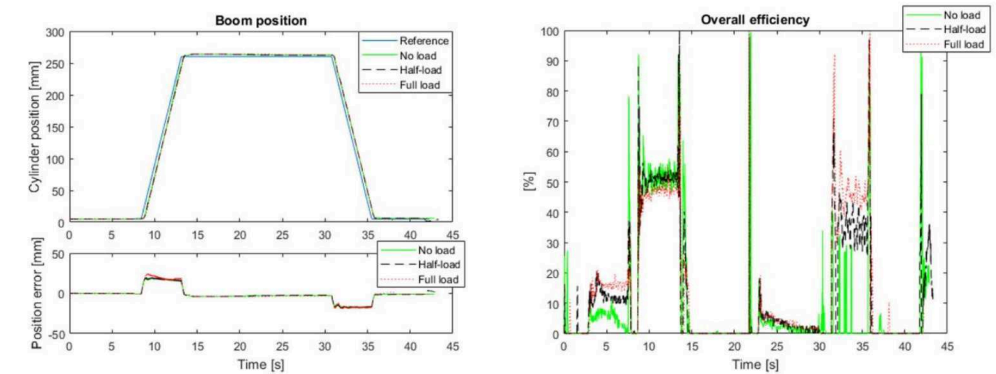


Figure 13: Experimental results: 1.7 \* nominal cylinder velocity – boom position reference tracking (left, up), boom position error (left, down) and efficiency (right) for different payloads

Proposed fuzzy PID controller demonstrated excellent self-adaptability with regard to various velocities and payloads (Figure 10 - Figure 13). The steady-state error was improved from 34 % to 1 % (from 88 mm to less than 3 mm), compared to the conventional PID control. In addition, the response time was shortened from 2 s to 0.3 s with proposed fuzzy PID controller. It can be seen from the position error graphs that the error caused by response time increases with cylinder velocity, but is almost identical for different payload cases. Furthermore, the overall system efficiency reaches the level of above 50 % (50 % - 60 % for cases of no load to half-load); while it is slightly lower in full load condition and varies in ranges 44 % - 50 % depending on velocity. It is significantly higher compared to conventional Load sensing (LS) systems, efficiency of which varies in the range of only 10 to 20 % /10/, /11/. It is noted that the power efficiency does not greatly depend on cylinder velocity. Moreover, as it was previously explained, during lowering motion of the boom, power regenerates. Regeneration efficiency is highest with full load (level of 48 % with normal cylinder velocity and 38 - 46 % in cases of other velocities); it decreases slightly with half-load (37 - 42 %), while it is insignificant in cases with no load. It can be concluded that regeneration efficiency depends on the payload, rather than cylinder velocity.

## 5 Discussion

This paper is dealing with the hybrid mining loader with zonal hydraulics realized with DDH. DDH is a compact hydraulic unit with low oil volume, short pipelines and reduced potential leakage points, which brings lower environmental hazards. In addition, regenerative energy of DDH brings advantages compared to conventional systems. This leads to extension of driving range and/or working time of electric driven vehicles. However, DDH itself requires a precise selection of hydraulic components to match hydraulic cylinder dimensions, and this brings along challenges with position control as system response directly depends on the electric motor.

In this research, reference tracking of the existing system was improved by means of automatization of the process of choosing PID controller parameters and keeping high efficiency of the system. For this purpose, a fuzzy PID controller was designed and implemented. In this paper, the positioning control in different loading conditions were implemented and verified experimentally with DDH mining loader, and thus, the goal of having a fuzzy PID controller independent from payload weight and velocity variation was reached.

However, fuzzy control also has some downsides. Its main disadvantage is that there is no general method (yet) of selecting parameters of membership functions for inputs and outputs or for defining the rules. Therefore, designing fuzzy control for each system requires excessive experimenting and testing. However, once the parameters and rules have been determined, it is fairly simple and straightforward to implement this type of control into a pre-existing model.

Despite demonstrated excellent performance and high efficiency, it is wise to note that a DDH unit comes with the price of extra electric components, such as an expensive battery, electric motors and controllers. In the future, dimensioning of components (due to unknown duty cycle), limited market of suitable and available electric components, as well as charging method and aging of battery should be considered. Regarding future research on the topic, position control of the bucket should be improved in order to increase power efficiency during the whole cycle.

## 6 Summary and conclusion

In order to investigate behaviour and efficiency of hybrid NRMM, a full-size prototype of a mining loader was built during the Tubridi and EL-Zon projects. The aim of this study was to improve reference tracking of the existing boom DDH system, while automating the process of choosing controller parameters and keeping the efficiency of the system as high as possible. For that purpose, a fuzzy PID controller was designed and implemented. The behaviour of the system was put to the test with three different payloads and with four distinct velocities. It is obvious that the reference tracking was significantly improved compared to the previous case when only a simple PID control was used – the steady-state error is noticeably reduced (from 34 % to around 1 %), and the response time is shortened (from 2 s to 0.3 s). Furthermore, the overall system efficiency reaches the level of above 50 % (50 % - 60 % for cases of no load to half-load); while it is slightly lower in full load condition (44 % - 50 %).

## 7 Acknowledgements

This research was enabled by the financial support of Tekes, the Finnish Funding Agency for Technology and Innovation (project EL-Zon) and internal funding at the Department of Mechanical Engineering at Aalto University.

## 8 Nomenclature

Variable	Description	Unit
$e$	Position error	[mm]
$\dot{e}$	Derivative of the position error	[mm/s]
$e(k)$	Error between the reference and the process output signal	[-]
$F_{boom}$	Force acting on load pins of the boom	[N]
$F_{bucket}$	Force acting on load pins of the bucket	[N]
$I_{boom}$	Battery output current that is used by the boom motor controller	[A]
$I_{bucket}$	Battery output current that is used by the bucket motor controller	[A]
$K_p$	Proportional gain	[-]
$K_i$	Integral gain	[-]
$K_d$	Derivative gain	[-]
$P_{bat}$	Battery output power	[W]
$P_{mech}$	Mechanical output power	[W]
$T_s$	Sampling period	[s]
$u(k)$	Control signal	[-]

$U_{bat}$	Battery output voltage	[V]
$v_{boom}$	Velocity of the boom cylinder	[m/s]
$v_{bucket}$	Velocity of the bucket cylinder	[m/s]
$\eta$	Overall system efficiency	[-]
$\eta_{reg}$	Regeneration efficiency	[-]

## References

- /1/ Georgescu, A., Prestidge, S., *Emissions from engines in non-road mobile machinery*, April 2015, [http://www.europarl.europa.eu/RegData/etudes/BRIE/2015/528820/EPRS\\_BRI\(2015\)528820\\_EN.pdf](http://www.europarl.europa.eu/RegData/etudes/BRIE/2015/528820/EPRS_BRI(2015)528820_EN.pdf)
- /2/ Tier 4 Emission Standards, <https://www.dieselnet.com/standards/us/nonroad.php#tier4>, visited on August 28, 2017.
- /3/ Hänninen, H., Minav, T., Pietola, M., *Replacing a constant pressure valve controlled system with a pump controlled system*, In: Proceedings of the 2016 Bath/ASME Symposium on Fluid Power and Motion Control, FPMC2016, Bath, United Kingdom, Sep 7-9, 2016.
- /4/ Minav, T., Lehmuspelto, T., Sainio, P., Tammisto, O., Pietola, M., *Series Hybrid Mining Loader with Zonal Hydraulics*, In: 10<sup>th</sup> International Fluid Power Conference, 10. IFK, Dresden, Germany, March 8-10, 2016.
- /5/ Zheng, J., Zhao, S., Wei, S., *Application of self-tuning fuzzy PID controller for a SRM direct drive volume control hydraulic press*, Control Engineering Practice, Volume 17, Issue 12, December 2009, Pages 1398-1404, available at: <http://www.sciencedirect.com/science/article/pii/S0967066109001336>
- /6/ Sinthipsomboon, K., Hunsacharoonroj, I., Khedari, J., Pongaen, W., Pratumsuwan, P., *A hybrid of fuzzy and fuzzy self-tuning PID controller for servo electro-hydraulic system*, In: 2011 6<sup>th</sup> IEEE Conference on Industrial Electronics and Applications (ICIEA), Beijing, China, Jun 21-23, 2011, available at: <http://ieeexplore.ieee.org/stamp/stamp.jsp?arnumber=5975583>
- /7/ Yu, L., Zheng, J., Yuan, Q., Xiao, J., Li, Y., *Fuzzy PID control for direct drive electro-hydraulic position servo system*, In: 2011 International Conference on Consumer Electronics, Communications and Networks (CECNet), Xianning, China, April 16-18, 2011.
- /8/ Sourander T., Pietola M., Minav T., Hänninen H., *Sensorless position estimation of simulated direct driven hydraulic actuators*, In: The 15<sup>th</sup> Scandinavian International Conference on Fluid Power, SICFP'17, Linköping, Sweden, June 7-9, 2017.
- /9/ Passino, K. M., Yurkovich, S., *Fuzzy control*, 1998 Addison Wesley Longman, Inc. Retrieved from: <http://www2.ece.ohio-state.edu/~passino/FCbook.pdf>
- /10/ Zhang S., Minav T., Pietola M., *Improving efficiency of micro excavator with decentralized hydraulics*, In: 2017 Bath/ASME Symposium on Fluid Power and Motion Control, FPMC 2017, Sarasota, Florida, USA, October 16-19, 2017.
- /11/ Zimmerman J. D., Pelosi M., Williamson C. A., Ivantysynova M., *Energy consumption of an LS excavator hydraulic system*, In: ASME 2007 International Mechanical Engineering Congress and Exposition, 117-126, Seattle, Washington, USA, November 11-15, 2007.